Adsorption of water monomer and clusters on platinum(111) terrace and related steps and kinks I. Configurations, energies, and hydrogen bonding

Líney Árnadóttir[a], Eric M. Stuve[a,*], Hannes Jónsson[b]

[a]*Department of Chemical Engineering, Box 351750, University of Washington, Seattle, WA 98195-1750*
[b]*Faculty of Science, VR-II, University of Iceland, 107 Reykjavík, Iceland*

Abstract

Adsorption and rotation of water monomer, dimer, and trimer on the (111) terrace, (221) and (322) stepped, and (763) and (854) kinked surfaces of platinum were studied by density functional theory calculations using the PW91 approximation to the energy functional. On the (111) terrace, water monomer and the donor molecule of the dimer and trimer adsorb at atop sites. The per-molecule adsorption energies of the monomer, dimer, and trimer are 0.30, 0.45, and 0.48 eV, respectively. Rotation of monomers, dimers, and trimers on the terrace is facile with energy barriers of 0.02 eV or less. Adsorption on steps and kinks is stronger than on the terrace, as evidenced by monomer adsorption energies of 0.46 to 0.55 eV. On the (221) stepped surface the zigzag extended configuration is most stable with a per-molecule adsorption energy of 0.57 eV. On the (322) stepped surface the dimer, two configurations of the trimer, and the zigzag configuration have similar adsorption energies of 0.55 ± 0.02 eV. Hydrogen bonding is strongest in the dimer and trimer adsorbed on the terrace, with respective energies of 0.30 and 0.27 eV, and accounts for their increased adsorption energies relative to the monomer. Hydrogen bonding is weak to moderate for adsorption at steps, with energies of 0.04 to 0.15 eV, as the much stronger water-metal interactions inhibit adsorption geometries favorable to hydrogen bonding. Correlations of hydrogen bond angles and energies with hydrogen bond lengths are presented. On the basis of these DFT/PW91 results, a model for water cluster formation on the Pt(111) surface can be formulated where kink sites nucleate chains along the top of step edges, consistent with the experimental findings of Morgenstern et al., Phys. Rev. Lett., 77 (1996) 703.

Keywords:
density functional theory, ab-initio simulation, water, platinum, terrace, step surface, kink surface, adsorption, hydrogen bond, cluster
PACS: 68.43.Bc, 68.43.Fg, 68.43Jk, 82.20.Pm, 82.30.Rs

1. Introduction

Water adsorption on late transition metals is a special and phenomenologically interesting case of substrate–adsorbate (SA) and adsorbate–adsorbate (AA) interactions being of similar magnitude. Such a case is distinct from chemisorption, characterized by strong SA bonds relative to AA bonds, or physisorption, characterized by weak SA bonds [1–3]. Values for the activation energy of water desorption from Pt(111) range from 0.44 to 0.56 eV [1, 4–6], in close agreement with the strength of two hydrogen bonds in water, 0.48 eV [7]. Studies of water adsorption and diffusion on late transition metals pertain to a molecular level description of the macroscopic phenomenon of wetting [8], which has received much attention [3]. Water adsorption illustrates the general case of similar SA and AA interactions, which has been compared with cases of SA-dominant or AA-dominant interactions by Pandit, Schick, and Wortis [9].

Monomeric or small clusters of water on Pt(111) have been studied by various experimental methods such as scanning tunneling microscopy (STM) [10–12], low energy electron diffraction (LEED) [5], and helium atom diffraction [6, 13]. Monomeric and small water clusters on metal surfaces are difficult to achieve experimentally due to rapid formation of larger clusters at temperatures as low as 60 K [6]. Despite these difficulties, several experimental studies of small water clusters and water diffusion on single crystalline surfaces have been performed [6, 10, 12, 14, 15]. Helium scattering studies of water diffusion on Pt(111) show that water adsorbs as monomers at temperatures below 40 K [16], becoming sufficiently mobile to form adsorbed clusters near 60 K [6].

Several recent density functional theory (DFT) calculations describe water interaction with various metal surfaces [17–22]. Michaelides et al. [18] studied monomer adsorption on various close-packed metal surfaces and found that water monomer binds at the atop site, tilting its hydrogen atoms 6–15° away from the surface. Meng, et al. [19] investigated small chains of water clusters, from monomer to hexamers, on stepped and terrace sites of Pt(111) and other close-packed metal surfaces. For adsorption on a stepped (322) platinum surface they found a chain of water molecules in a "zigzag" configuration to be the most stable. Grecea, et al. [23] studied water on Pt(533)

*Corresponding author
Email addresses: lineya@u.washington.edu (Líney Árnadóttir), stuve@u.washington.edu (Eric M. Stuve), hj@hi.is (Hannes Jónsson)

and found that a monomer has the strongest surface interaction at the step edge, with decreasing surface interaction as the monomer moves down from the step and out onto the terrace.

In this paper we use DFT and the PW91 functional to examine water adsorption on a Pt(111) terrace, (221) and (322) stepped surfaces, and (763) and (854) kinked surfaces. The adsorption energy and configurations of water monomer, dimer, and trimer were examined. The goal of this work was to learn about the energy landscape that governs the initial formation of water clusters on the Pt(111) surface, in particular the role of kinks and steps, and see whether the DFT/PW91 approximation is consistent with the available experimental data. Furthermore, the role of hydrogen bonds *vs.* water-metal bonds in small clusters is addressed.

2. Methodology and Systems of Study

2.1. Computational Parameters

All calculations presented here were done with the Vienna *ab-initio* simulation package (VASP), a plane-wave implementation of DFT with the PW91 functional [24–28]. Interactions between ions and electrons were described by ultra-soft Vanderbilt pseudopotentials (US-PP) [29, 30]. The recommended cut-off energy for oxygen, 396 eV (29 Ry), was used for all calculations, and the Brillouin zone was sampled with a $2 \times 2 \times 1$ Monkhorst-Pack k-point mesh. A $4 \times 4 \times 1$ Monkhorst-Pack k-point mesh reproduced the results of the $2 \times 2 \times 1$ mesh to within 3 meV for binding energies. The calculations were considered converged when the maximum forces on all relaxed atoms were less than 50 meV/Å for adsorption on kinked and stepped surfaces, for adsorption of extended configurations, and for nudged elastic band calculations; and 10 meV/Å for all other calculations. The rate and mechanism of water monomer and dimer rotation on Pt(111) were determined by the climbing image, nudged elastic band (cNEB) method [31, 32].

The calculated lattice constant for platinum was found to be 3.98 Å, in good agreement with the experimental value of 3.924 Å [33]. The surface was cut out of a previously relaxed Pt-bulk and relaxed again keeping only the bottom layer fixed. The vacuum layer was 15 Å. Only the adsorbed molecules were allowed to relax during the calculations.

Recently, Santra et al. [34], examined the ability of various DFT functionals to describe hydrogen bonds in small water clusters. With reference to Møller-Plesset perturbation theory (MP2), the PW91 functional yielded dimer and trimer hydrogen bond strengths within 17 meV of the MP2 benchmark. In another comparison, again against the MP2 benchmark, the PW91 functional yielded hydrogen bond strengths within 26 meV for hydrogen bonding in DNA base pairs [35]. From these studies, relying more on the comparison with water clusters, we conclude that hydrogen bond strengths reported here can be compared at differences of 20 meV or greater.

The adsorption energy per water molecule was calculated by comparing the total energy of n number of isolated water molecule(s) in the gas phase E_w and the energy of the clean surface E_{surf} to the total energy of an adsorbed cluster of n water molecules $E_{tot,ads}$, according to Eq. 1:

$$E_{ads} = \frac{1}{n}\left[E_{tot,ads} - (E_{surf} + nE_w)\right], \quad (1)$$

The quantity E_{ads} is a per-molecule quantity that includes the effects of metal–water and water–water hydrogen bonds, the latter expressed as an average value for each hydrogen bond in the cluster. The zero-point energy correction for the adsorption energy (ΔZPE) was calculated as the difference between the ZPE correction of the adsorbate on the surface and in the gas phase according to Eq. 2:

$$\Delta ZPE = \left(\sum_{i=1}^{3n} \frac{\hbar\omega_i}{2}\right)_{surf} - \left(\sum_{i=1}^{3n} \frac{\hbar\omega_i}{2}\right)_{gas}. \quad (2)$$

2.2. Configurations

Figure 1 shows the structure of the five surfaces examined in this work, along with the unit cells (solid lines) and calculated cells (dashed lines). For the kink surfaces, the calculated cell is the same as the unit cell. The unit cells are positioned to show the adsorption sites for water. Calculations on the flat Pt(111) surface were performed with a total of 36 substrate atoms: 12 atoms per layer in three layers. Step sites were each represented by 3×5 surface atoms in 4 layers for all calculations of water monomer and single-sided chains on step edges. A larger unit cell, 4×5 surface atoms in 4 layers, was needed to fulfill the periodic boundary conditions requirement for the zigzag chains; the larger cell was also used for the water clusters. No significant differences were found between the two calculated cell sizes. Kink sites were represented by 3×4 surface atoms in 5 layers.

The (763) and (221) surfaces have (111)-oriented edges, which are referred to as type-A steps. The (763) surface has (100)-oriented kinks. The (854) and (322) surfaces have (100)-oriented edges, which are referred to as type-B steps. The (854) surface has (111)-oriented kinks. Table 1 lists size and minimum water coverage for the five surfaces.

The minimum energy sites for water adsorption, as determined from the DFT calculations discussed below, are also depicted in Fig. 1. Including all of the adsorption configurations in one figure facilitates comparison among the different cases.

Table 1: Surface designation, unit cell area A_u, calculated cell area A_{calc}, and minimum calculable water coverage $\theta_{w,min}$ for the surfaces shown in Fig. 1. The minimum water coverage is that of one water molecule within a calculation cell. Areas are given in terms of d^2, where d is the nearest neighbor distance in the crystal. For Pt the value of d is 2.77 Å.

Surface	Type	A_u/d^2	A_{calc}/d^2	$\theta_{w,min}$ / ML
(111)	Terrace	0.866	10.392	0.083
(221)	Step-A	3.000	9.000	0.096
(322)	Step-B	4.123	16.492	0.052
(763)	Kink-A	9.695	9.695	0.089
(854)	Kink-B	10.247	10.247	0.084

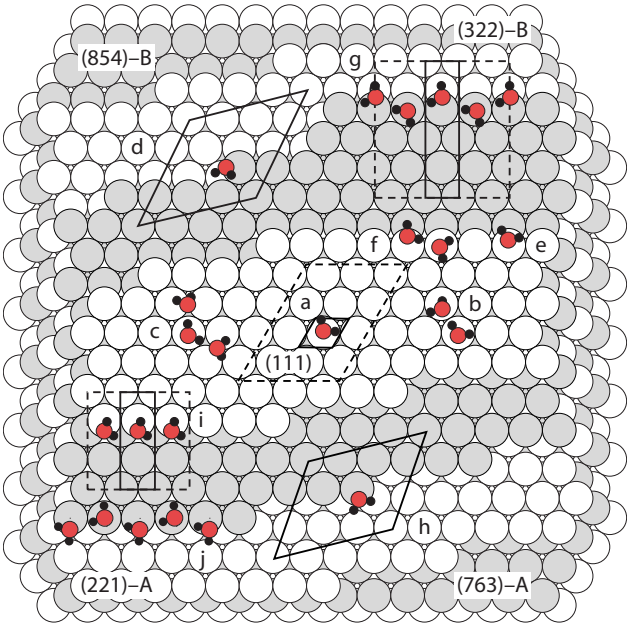

Figure 1: Illustration of the five surfaces cut from a FCC crystal. The (111) plane is shown in the center. Beginning from the top left and proceeding clockwise, the surfaces, as shown, are (548), (223), (673), and (221). Since the order of the indices does not matter for cubic crystals, the surfaces are labeled (854), (322), (763), and (221). Also shown are minimum energy sites for water: (a) monomer on (111); (b) dimer on (111); (c) trimer on (111); (d) monomer at (854) (kink-B); (e) monomer at (322) (step-B); (f) dimer at (322) (step-B); (g) zigzag configuration at (322) (step-B); (h) monomer at (763) (kink-A); (i) chain configuration at (221) (step-A) and (j) zigzag configuration at (221) (step-A). Solid lines show unit cells of each surface. Dashed lines show the calculated cells for each surface. For the kink surfaces the calculated cell is the same as the unit cell.

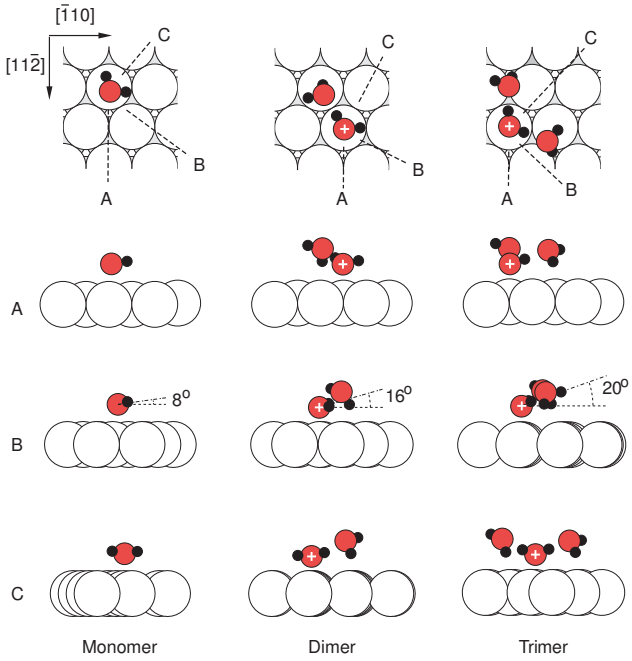

Figure 3: Adsorption orientation and hydrogen bonding of water monomer, dimer, and trimer on Pt(111). Hydrogen bond donor molecules are signified by a white cross. The other cluster molecules are hydrogen bond acceptors. Top row: view normal to the surface of adsorbed monomer (left), dimer (center), and trimer (right); the dashed lines A, B, and C show the directions of respective views in the lower rows. (A): view in the (111) plane (along the [$\bar{1}\bar{1}$2] direction) of the respective clusters. (B): view normal to the plane bisecting the ∠HOH angle, showing the donor tilt angle. (C): view along the plane bisecting the ∠HOH angle, showing hydrogen bonding.

The configurations and adsorption sites are discussed in more detail below.

3. Results

3.1. Water adsorption on the Pt(111) terrace

The lowest energy configurations for water monomer, dimer, and trimer on Pt(111) are shown in Figs. 2 and 3. Figure 2 shows enlarged views of the adsorption configurations, and Fig. 3 shows orientation and hydrogen bonding. Adsorption occurs with at least one molecule at an atop site. In the case of the dimer and trimer, the molecule that is the hydrogen bond donor is signified by the white cross. Monomer water is nearly parallel to the surface, with a tilt angle of 8°. The tilt angle increases in the dimer (16°) and trimer (20°), indicating that increasing hydrogen bonding pulls water away from its monomer orientation. The acceptor molecules are twisted such that one of the hydrogen atoms points toward the surface, while the other points away from it.

Table 2 lists structural data for all systems studied. The O–Pt distance for monomer adsorption on Pt(111) of 2.34 Å will be used as a basis for comparison with the other adsorption systems. The O–Pt distances of dimer and trimer donor molecules on Pt(111) range from 2.18 to 2.37 Å, corresponding to deviation from the monomer by −6.8% to +1.3%. The O–Pt distance of the monomer is exceeded only by the deuterated monomer, so the O–Pt distances of dimer and trimer clusters are all smaller than that of the monomer.

The O–Pt lengths of acceptor molecules are considerably greater, ranging from 3.09 to 3.46 Å. The trimer-ring structure, in which each molecule serves as donor and acceptor, has O–Pt distances of 3.40 to 3.60 Å, indicating that these molecules adsorb more as acceptors than as donors.

Hydrogen bond lengths are short compared to the gas phase value of 1.96 Å for the dimer. They have a narrow range from 1.61 Å to 1.68 Å. The hydrogen bonds are unconstrained, as their angles of 175 to 179° are close to the gas-phase dimer value of 171°. These results are in good agreement with water adsorption sites and configurations found in previous calculations [18, 19, 36, 37].

Adsorption energies for all systems studied are listed in Table 3. The adsorption energy for water monomer on the flat terrace was found to be 0.30 eV. An interesting point is that the adsorption energy per water molecule increases with increasing cluster size to 0.45 eV for the dimer and 0.48 eV for the trimer. The monomer and dimer adsorption energies agree with earlier work [18, 19]. The trimer results differ, however, in that Meng et al. [19] reported a ring structure as the lowest energy struc-

Table 2: Structural parameters for water molecules and clusters adsorbed on terrace, step, and kink sites on Pt: H_2O–Pt length, H–O–H angle ∠(HOH), hydrogen bond length, and hydrogen bond angle ∠(O–H$\cdots$O). Hydrogen bond (H-bond) mode classifies entries in terms of donor molecules (D) and acceptor molecules (A). Note that each water molecule is both a donor and acceptor in the chain and zigzag configurations. The order of entries in the ∠(HOH), H-bond length, and H-bond angle columns corresponds to the order in the H_2O–Pt length column. Entries in italics are values from the literature. Literature values for the gas phase dimer are taken from refs. [34, 38–41].

	H_2O–Pt length [Å]				H–O–H angle ∠(HOH) [°]			H-bond length OH$\cdots$O [Å]			H-bond angle ∠(O–H$\cdots$O) [°]		Fig.
H-bond mode	D	A	D	A									
Gas phase													
Dimer					105			1.86			176		
Dimer								*1.96*			*171*		
Trimer					105			1.95	1.97		178	175	
Terrace													
Monomer	2.34				105.7								3
D-monomer	2.37												
Monomer [18]	*2.36*				*106*								
Monomer [19]	*2.40*				*105.6*								
Dimer	2.20	3.18			107	104		1.61			178		3
D-dimer	2.24	3.18						1.64			179		
Dimer [19]	*2.26*	*3.05*			*106.7*			*1.69*					
Trimer-row		3.29	2.18	3.46	105	107	104	1.68	1.66		175	178	3
D-trimer-row		3.09	2.18	3.17				1.68	1.66		176	178	
Trimer-ring	3.40	3.50	3.60		106.7	106.8	106.2	1.78	1.84	1.87	150	151	
Trimer-ring [19]	*2.76*	*2.76*	*2.76*		*107.8*			*1.795*	*1.815*	*1.805*			
Type-A step													
Monomer	2.31				106.4								
Dimer	2.28	2.58			107.4	106.8		1.80			163.1		
Trimer-row	2.33	2.63		2.44	106.2	106.0	106.6	1.90	1.85		162.9	167.2	4A
Trimer-open		3.20	2.18	2.64	105.0	107.7	105.2	1.69	1.69		174.7	178.0	4B
Chain		2.52		2.52	104.1	104.1		1.96	1.99		141.9	140.8	4C
Zigzag	2.47	2.50			105.6	105.8		2.03	2.03		163.0	163.4	
Type-B step													
Mono. H-out	2.36				105.7								4F
Mono. H-in [19]	*2.22*												
Mono. H-out [19]	*2.25*												
Dimer	2.22	2.90			107.7	105.2		1.72			170.9		4E
Trimer-row	2.28	2.71		2.33	107.2	103.5	106.7	1.78	1.62		161.2	176.4	
Trimer-open		3.06	2.16	3.17	105.8	106.8	105.4	1.70	1.65		177.2	173.1	
Chain		2.48		2.48	104.5	104.5		1.96	1.96		144.5	144.5	
Zigzag	2.47	2.64			105.5	105.3		2.01	1.96		163.1	165.3	4D
Zigzag [19]	*2.62*	*2.72*											
Kinks													
A-Mono. H-out	2.30				105.6								4H
B-Mono. H-in	2.44				105.3								4G

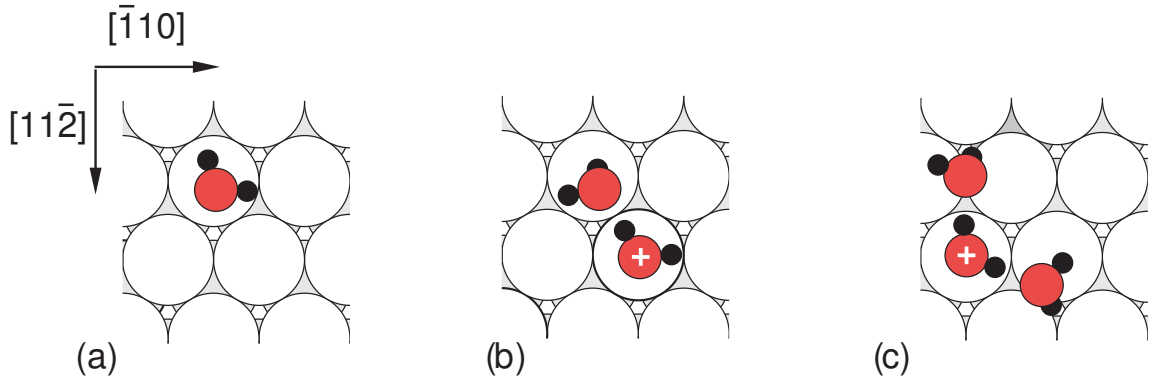

Figure 2: Monomer (a), dimer (b), and trimer (c) adsorption on Pt(111). Hydrogen bond donor molecules are signified by a white cross.

ture, while our results give lower energy for an open structure. An open trimer structure has also been found to be more stable than a ring structure on Cu(111) [42].

3.2. Adsorption on steps and kinks

Figure 4 shows configurations of water molecules, clusters, and extended configurations adsorbed at step and kink sites. Here, clusters are defined as small assemblies of water molecules that are neither cyclic nor extended in nature, exemplified by the dimer, trimer-row, and trimer-open structures of this study. Extended configurations span many unit cells of the surface and include the chain and zigzag structures studied here. Each water molecule in an extended configuration serves as hydrogen bond donor and acceptor. As each water molecule in a cyclic structure also has donor and acceptor character, a cyclic structure–in this case the trimer-ring–is a special case of an extended configuration.

In general, water adsorption at atop sites is preferred. At least one water molecule in each cluster adsorbs atop a step edge atom. An exception is the low energy chain configuration on step A, Fig. 4C, in which there is no atop adsorption. Monomer adsorption at kink sites is not atop, however, no doubt due to the unique electronic structure of the kink site.

The O–Pt distance for monomer adsorption varies little among terrace, step, and kink sites. Values range from 2.30 Å for adsorption at kink-A to 2.44 Å for adsorption at kink-B, corresponding to a range of −1.7% to +4.3% relative to the monomer/terrace basis. It is interesting that, despite the stronger bonding of water to step and kink sites (Table 3), their O–Pt distances are both below and above that of the terrace monomer. Thus, O–Pt distance and adsorption energy have no simple correlation.

The O–Pt distances of donor molecules in dimer and trimer clusters also have a small range from 2.16 to 2.33 Å, corresponding to a difference of −7.7% to −0.4% relative to the monomer/terrace basis. Acceptor O–Pt distances are larger and range from 2.33 to 3.20 Å, which is sufficient to distinguish O–Pt distances of acceptors from those of donors. In the chain and zigzag extended configurations each molecule functions as both donor and acceptor, yet the range of O–Pt distances of 2.47 to

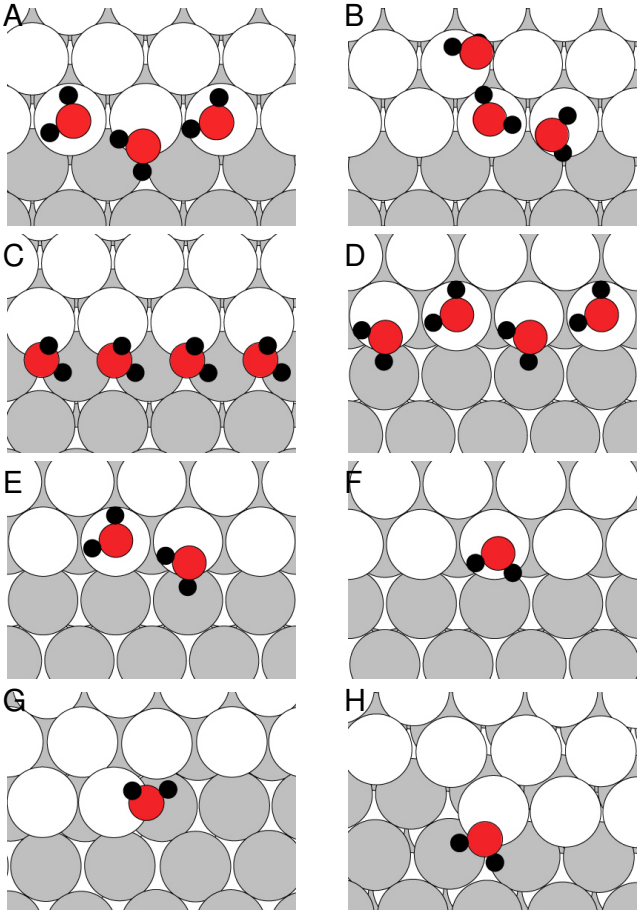

Figure 4: Examples of step and kink configurations: (A) trimer row on step-A; (B) trimer-open on step-A; (C) single-sided chain on step-A; (D) zigzag chain on step-B; (E) dimer on step-B; (F) H-out monomer on step-B; (G) H-in monomer on kink-B; and (H) H-out monomer on kink-A.

Table 3: Adsorption energy per molecule E_{ads}, average energy per hydrogen bond E_H determined from Eq. 4, ratio of adsorbate-adsorbate to substrate-adsorbate energies AA/SA as defined in Eq. 6, and zero point energy difference determined from Eq. 2, for water molecules and clusters adsorbed on terrace, step, and kink sites of Pt. Entries in italics are values from the literature.

	$-E_{ads}$ [eV]	$-E_H$ [eV]	AA/SA	ΔZPE [eV]
Gas phase				
Dimer		0.27		
Dimer [40, 41]		*0.22*		
Trimer		0.22		
Terrace				
Monomer	0.30			−0.04
D-monomer	0.30			0.09
Monomer [18]	*0.35*			
Monomer [19]	*0.30*			
Dimer	0.45	0.30	0.50	0.07
D-dimer	0.44	0.28	0.47	0.06
Dimer [19]	*0.43*	*0.26*	*0.42*	
Trimer-row	0.48	0.27	0.60	0.03
D-trimer-row	0.47	0.26	0.57	0.1
Trimer-ring	0.45	0.15	0.50	0.01
Trimer-ring [19]	*0.36*	*0.06*	*0.18*	
Step-A				
Monomer	0.47			0.05
Dimer	0.53	0.12	0.13	0.05
Trimer-row	0.51	0.08	0.11	0.04
Trimer-open	0.52	0.07	0.10	0.04
Chain	0.44	−0.03	−0.06	0.02
Zigzag	0.57	0.10	0.21	0.03
Step-B				
Monomer H-out	0.46			0.05
Mono. H-in [19]	*0.45*			
Mono. H-out [19]	*0.43*			
Dimer	0.53	0.14	0.15	0.05
Trimer-row	0.56	0.15	0.22	0.07
Trimer-open	0.54	0.12	0.18	0.04
Chain	0.50	0.04	0.09	0.002
Zigzag	0.55	0.09	0.20	0.09
Zigzag [19]	*0.48*	0.03	0.07	
Kinks				
A-Mono., H-out	0.51			0.06
B-Mono., H-in	0.55			0.06

2.64 Å falls within the range of acceptor O–Pt distances in the clusters.

Hydrogen bond lengths are generally larger for adsorption on step and kink sites relative to terrace sites. For clusters on steps and kinks, hydrogen bond lengths range from 1.62 to 1.90 Å, significantly larger than those for terrace clusters yet shorter than the gas phase value. For extended configurations the range in hydrogen bond lengths is 1.96 to 2.03 Å, essentially the same as the gas phase value. There is a clear distinction between the cluster and extended configurations with respect to hydrogen bond lengths.

Hydrogen bond angles generally fall within the range of 161.2 to 178.0°. The only exceptions are the chain configurations, which have hydrogen bond angles of 140.8 to 144.5°, consistent with their weak hydrogen bonds (discussed below).

Water monomer binds ≈ 0.16 eV more strongly to a step site than to a terrace site, while binding to a kink site is more than 0.2 eV stronger than to a terrace site (see Table 3). Adsorption at kink sites is so strongly preferred that a monomer at a kink site has the same adsorption energy per molecule as clusters on step sites and a greater adsorption energy than clusters on the terrace. It is interesting to note that, with the exception of the chain configuration on step-A, the per-molecule adsorption energies for clusters on type A and B steps are effectively equivalent.

There are two configurations for a monomer on steps: one with the hydrogens pointing towards the upper terrace (H-in) and the other with the hydrogens pointing towards the lower terrace (H-out). Our calculations for step-B found the H-out configuration (Fig. 4D) to be the most stable. Meng et al. [19] first reported these configurations and found H-in to be more stable by 0.02 eV. This energy difference is small, and we conclude that our finding in favor of the H-out configuration does not represent significant inconsistency with the earlier work [19].

We also found a small energy difference for H-in *vs.* H-out adsorption at kink sites. A water molecule adsorbed at kink-B has a slightly larger adsorption energy in the H-in configuration (Fig. 4G) than in the H-out configuration, although the difference is barely significant (about 0.04 eV). The opposite case is observed for adsorption at kink-A (Fig. 4H) for which the lowest energy configuration is H-out.

The per-molecule adsorption energies of dimers and trimers adsorbed on the steps fall in the range of 0.52 to 0.56 eV, with the exception of the value of 0.44 eV for the extended chain configuration on step-A. There is a 14% increase in adsorption energy in going from the monomer (0.46, 0.47 eV) to the dimer (0.53 eV), but no further increase in larger configurations, both cluster and extended. Again, the chain configuration on step-A is the anomalous result.

Of the extended configurations the zigzag configuration is most stable on both step-A and step-B. On step-A the energy difference relative to the chain configuration is considerable, 0.13 eV, while on step-B the difference is smaller, 0.05 eV, but large enough to assign the zigzag structure as the most stable. Meng et al. [19] also found in favor of the zigzag structure on step-B.

3.3. Hydrogen bonding in adsorbed water

Hydrogen bond strengths in adsorbed water were estimated by comparing the adsorption energy of the water configuration with that of an equivalent number n of adsorbed, non-interacting water molecules. The effective chemical reaction for this estimate is,

$$n\,\mathrm{H_2O_{ads}} \rightarrow (\mathrm{H_2O})_{n,\mathrm{ads}}. \tag{3}$$

The average, single hydrogen bond strength E_H is given by

$$E_H = \frac{n}{n_H}(E_{ads} - E_{ads,m}), \tag{4}$$

where

$$\begin{aligned} n_H &= n - 1 \quad \text{for finite clusters} \\ &= n \quad \text{for extended or cyclic configurations,} \end{aligned}$$

and $E_{ads,m}$ is the adsorption energy of the monomer on the same substrate. In this definition all hydrogen bonds in the configuration are assumed to have the same strength E_H, hence E_H represents the average hydrogen bond energy. This definition is equivalent to that of Meng et al. [19] and to the second case (Eq. 5) of Michaelides et al. [17].

The adsorption energy contains both hydrogen bonding (AA) and SA interactions. The AA interaction is given by the cumulative hydrogen bond strength $n_H E_H$ in the configuration, while the SA interaction nE_{SA} is given by the cumulative adsorption energy of the configuration less the AA interactions,

$$nE_{SA} = nE_{ads} - n_H E_H = nE_{ads,m}, \tag{5}$$

from which it can be shown that

$$\frac{AA}{SA} = \frac{n_H E_H}{nE_{SA}} = \frac{E_{ads}}{E_{ads,m}} - 1. \tag{6}$$

Hydrogen bond strengths and AA/SA ratios calculated by Eqs. 4 and 6 are listed in Table 3.

Hydrogen bonding is strongest for dimer and trimer clusters on the terrace. Values range from 0.26 eV for the deuterated trimer to 0.30 eV for the dimer and exceed the literature value of 0.22 eV for the gas phase dimer. The value for the dimer of 0.30 eV is in reasonable agreement with that of 0.26 eV reported by Meng et al. [19]. The AA/SA ratios are also highest for the cluster/terrace systems, ranging from 0.47 to 0.60. For adsorption on terraces, hydrogen bonding is an important component of the adsorption energy, representing approximately one-third the total adsorption energy.

Hydrogen bonds exert a minor influence in clusters at type-A steps and a moderate influence in those at type-B steps. (The anomalous value for the chain configuration on step-A is excluded from this analysis.) Accordingly, the AA/SA ratios are small for adsorption at step sites. We conclude that water adsorption at step sites is dominated by water–metal interactions with little or no influence of hydrogen bonds.

3.4. Rotation of water molecules on Pt(111)

Since water adsorbs at an atop site with the plane of the molecule nearly parallel to the surface, we anticipate that the rotational barrier will be small. Indeed, the barrier for rotation of the monomer about the surface normal is just 0.01 eV. For the dimer and trimer, rotation occurs about the surface normal axis of the donor oxygen atom, also with a small barrier of 0.02 eV. In all three cases the water molecules maintain the O–Pt distances of their most stable configurations. This low barrier of rotation for both dimer and trimer suggests a weak interaction between the lower hydrogen of the acceptor molecules and the surface (see Fig. 3). Facile rotation of water molecules has also been seen in calculations on Pt(111) and Pd(111) [18] and Al(100) [21, 43, 44].

Figure 5 shows an overlay of five images of dimer rotation. Durning the rotation the donor molecule moves less then 0.02 Å in the [111] direction but about ±0.2 Å in the (111) plane for the dimer, while both the monomer and the trimer and show little shifts in the (111) plane.

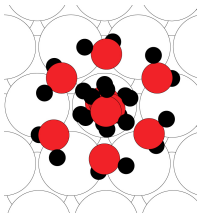

Figure 5: Rotation of water dimer on an atop site on Pt(111). The energy barrier for this rotation is very low, 0.02 eV.

4. Discussion

4.1. Water adsorption and configuration

4.1.1. Structural Parameters

It is possible to correlate the bond lengths listed in Table 2 to obtain an overall description of adsorption configurations, especially the relationships of O–Pt and hydrogen bond lengths for adsorption on terrace and step/kink sites. Figure 6 shows O–Pt distances and hydrogen bond lengths grouped according to adsorption at terrace sites; at step and kink sites; and for the ring, chain, and zigzag extended configurations. There are three regions of bond lengths: (1) hydrogen bond lengths of 2.1 Å and less, (2) O–Pt distances of monomers and donor molecules of 2.18–2.44 Å, and (3) O–Pt distances of acceptor molecules of 2.33 Å and greater.

Within the hydrogen bond group, bond lengths are smallest for terrace adsorption and greatest for the extended configurations. Hydrogen bond lengths for adsorption at steps and kinks are intermediate of the terrace and extended configurations. The groupings reveal that hydrogen bonding is strongest for terrace, variable from strong to weak for steps and kinks, and weak in the extended configurations.

The O–Pt distances for monomers and donors fall into a tight range. This indicates that the metal–oxygen interactions for

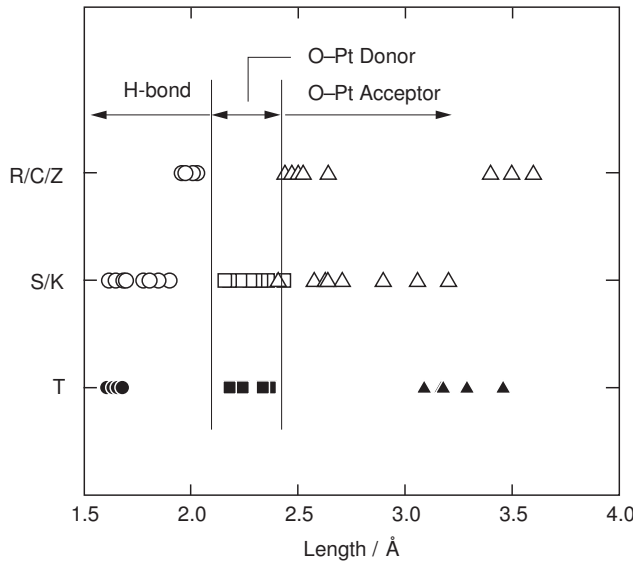

Figure 6: Distribution of bond lengths for adsorption of water at terrace sites (T), step and kink sites (S/K), and in ring/chain/zigzag (R/C/Z) configurations on a Pt surface. The results fall into three groups: hydrogen bond lengths (circles), O–Pt distances in donors (squares), and O–Pt distances in acceptors (triangles). Filled symbols are for terrace sites. Open symbols are for steps, kinks, and extended configurations.

these systems are all approximately similar, despite differences in adsorption geometry and hydrogen bonding.

For acceptor molecules, the O–Pt distances fall in a wide range that includes two sub-groups. The first sub-group consists of acceptors at steps and kinks and in chain and zigzag configurations with O–Pt distances ranging from 2.33 to 3.20 Å, indicating a moderate metal–oxygen interaction in these molecules. The second sub-group includes all terrace adsorption and the trimer-open structures with greater O–Pt distances ranging from 3.09 to 3.60 Å. Compared to acceptors at steps and kinks and in extended configurations, the configurations in the terrace group have weaker metal–oxygen interactions and therefore rely more on hydrogen bonding for their stability.

4.1.2. Adsorption energies

For monomer *vs.* cluster adsorption the largest difference in adsorption energies occurs for terrace sites. The per-molecule adsorption energies of the dimer and trimer are at least 50% greater than that of the monomer. That the monomer should have a low adsorption energy is well known [3]. The difference comes about by hydrogen bonding in the dimer and trimer, which we will discuss further in Sec. 4.2.

For adsorption on step sites the difference between monomers and clusters in regards to adsorption energy is less. The range of adsorption energies of dimers and trimers at steps of 0.52 to 0.56 eV is approximately 16% greater than that of monomers at steps, 0.46 and 0.47 eV. The difference between steps and terrace in this regard arises from the stronger bonding of water to the lower coordinated substrate atoms of steps.

Meng et al [19] studied a subset of the configurations reported here. Within that subset, the primary difference from our work regards the most stable trimer structure on the terrace. Our calculations find in favor of an open structure, which has an adsorption energy of 0.03 eV per molecule greater than that in our calculation of the ring structure. The earlier calculations differ substantially from ours, yielding smaller O–Pt distances (2.76 *vs.* 3.40 Å), smaller adsorption energies (0.36 *vs.* 0.45 eV), and smaller hydrogen bond energies (0.06 *vs.* 0.15 eV). The reasons for the discrepancies are likely due to different surface coverages studied in the calculations.

It is interesting to note the similarities of adsorption energies of the various configurations on step surfaces. On step-A the zigzag structure is preferred by 0.04 eV, large enough to favor that structure. On step-B, however, adsorption energies of the dimer, trimer-row and trimer-open, and zigzag structures fall within the range of 0.55±0.02 eV, a difference too small to make a definitive conclusion of one configuration over the other. With such similar adsorption energies any of these structures could exist on B-type steps.

The strong preference for water adsorption on steps and kinks is in a good agreement with experimental work. The STM studies of Morgenstern and coworkers [10] found that low coverage water aligns along step edges rather than on the terrace. There was also a difference between the two types of steps, where, on step-A, water molecules formed long one-dimensional chains, while on step-B, water formed smaller, isolated chains. Grecea, et al. [23] found significantly higher desorption energy for water at step edges and terraces of a Pt(533) surface. Water binds most strongly at the step edge, with decreased desorption energy at terrace sites. The desorption energy for the terrace sites of the stepped surface was markedly greater than that for desorption from a flat Pt(111) surface.

4.2. The hydrogen bond in submonolayer water

4.2.1. Definition of the hydrogen bond energy

In this section we discuss possible definitions of the hydrogen bond energy in adsorbed water. In Eq. 4 all hydrogen bonds within the adsorbed complex are assumed to have the same strength E_H. There are two conceptual difficulties with this definition. First, there is no reason to expect that multiple hydrogen bonds within an adsorbed complex should have the same strength. While some clusters, such as the terrace trimer, have nearly equivalent hydrogen bond lengths, others, such as the step-B trimer-row, do not. It is reasonable to assume similarity of hydrogen bond strengths in the terrace trimer, but little reason to do so in the step-B trimer. The second difficulty is that hydrogen bonding in adsorbed complexes cannot be distinguished from metal–water interactions; the two are comingled. As it represents both hydrogen bonding and metal–water interactions, the energy E_H is more accurately described as an overall cohesion energy of the adsorbed complex. Nonetheless, we prefer the term hydrogen bonding as the effects seen in this study fit well within the sense of hydrogen bonding as applied to water. The distinction between metal–water and adsorbate–adsorbate interactions is discussed further below.

The definition in Eq. 4 references only the adsorbed cluster and monomer states, both accessible experimentally as shown

by the potential energy surface for dimer adsorption in Fig. 7. From left to right, gas phase water molecules (a) adsorb as monomers (b), which then combine to form an adsorbed dimer (d). For adsorption on Pt(111) the total energy change for this process is twice the per-molecule adsorption energy, or −0.90 eV. The hydrogen bond energy, given by Eq. 4 and shown as E_H in the figure, is the difference between the monomer and dimer adsorption energies.

An alternative definition of hydrogen bond strength can be defined on the basis of a virtual reference state on the potential energy surface. The virtual reference state (c) consists of two, non-interacting water molecules in the same configuration as the lowest energy dimer (d). The motivation for this definition is to isolate adsorbate–adsorbate (hydrogen bonding) interactions from metal–water interactions. The hydrogen bond strength so defined is denoted as $E_{H,s}$. The subscript s signifies a virtual reference state with only substrate interactions. From Fig. 7 we obtain the following expressions for $E_{H,s}$ and E_H

$$E_{H,s} = 2E_{ads} - E_s \tag{7}$$

$$E_H = E_{H,s} + E_s - 2E_{ads,m} \tag{8}$$

where E_s is the energy of two non interacting water molecules in the dimer configuration (c). Since state (b) represents the minimum energy configuration for adsorbed monomers, it follows that state (c) must be of higher energy, hence

$$E_s \leq 2E_{ads,m}. \tag{9}$$

Substitution of this result into Eq. 8 gives

$$E_H \leq E_{H,s}. \tag{10}$$

Thus, hydrogen bond strengths referenced to the virtual state (c) exceed those referenced to non-interacting molecules in their lowest energy configuration (b). For the example of dimer adsorption on Pt(111), we calculated the value of $E_{H,s}$ to be 0.32 eV, from which we conclude that the energy penalty for bringing two non-interacting monomers into the non-hydrogen bonded dimer configuration (c) is 0.02 eV. Combination of the two values (with appropriate signs) gives the experimentally accessible hydrogen bond energy of 0.30 eV, listed in Table 3.

In separating structural from adsorbate–adsorbate effects, the virtual reference state largely decouples metal–water interactions from hydrogen bonding. The separation is not complete, however, in that addition of hydrogen bonding in the calculation from state (c) to (d) could alter metal–water interactions. This effect should be of second order, so the hydrogen bond energy based on the virtual reference state $E_{H,s}$ is the preferred method for assessing hydrogen bond energy apart from water–metal interactions.

A potential problem with hydrogen bonds referenced to the virtual state is that they may be subject to inconsistency. In the case of trimer adsorption, for example, one would compute the strength of the first hydrogen bond $E_{H,s1}$ as the difference in energy between a trimer with one hydrogen bond relative to the adsorbed, non-hydrogen bonded trimer. From there, the calculation proceeds to obtain the second hydrogen bond $E_{H,s2}$. Alternatively, one could reverse the order and compute $E_{H,s2}$ first

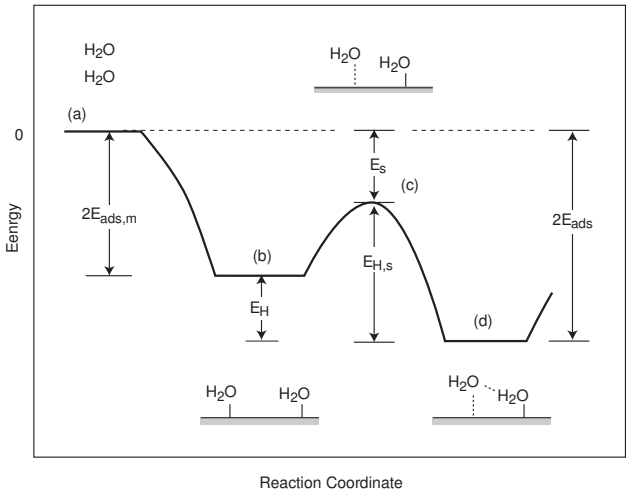

Figure 7: Potential energy surface for formation of an adsorbed dimer from gas phase water molecules. The molecular complexes are: (a) gas phase water molecules; (b) adsorbed, non-interacting monomers; (c) adsorbed, non-interacting water molecules in the same configuration as the lowest energy dimer (d); and (d) the lowest energy adsorbed dimer. See text for further details.

and then $E_{Hs,1}$. If any interdependence of metal–water interactions and hydrogen bonding exists, there is no reason to expect the bond strengths to be the same when computed in different orders. The value of the virtual reference state is its ability to isolate hydrogen bonds from metal–water interactions. When used for structures more complex than dimers, the method is subject to inconsistency. Unfortunately, the virtual reference state is not accessible experimentally so that results can only be compared among other calculations.

4.2.2. Hydrogen bonds in clusters and extended configurations

The systems studied exhibited a wide range of hydrogen bond strengths, from −0.03 to 0.30 eV, for a variety of substrates and configurations. It is possible to correlate hydrogen bond strength with both substrate and configuration, as shown in Fig. 8. Hydrogen bond angle, Fig. 8(a), and hydrogen bond length are correlated such that the shortest bond lengths, approaching 1.6 Å, have angles near 180°, whereas longer bond lengths of approximately 2.0 Å correlate with smaller bond angles of 140° to 150°. Hydrogen bond strength, Fig. 8(b), also correlates with bond length, such that the strongest hydrogen bonds, 0.30 eV, occur with the shortest bond lengths. Hydrogen bond strength falls to small values at the longest bond lengths. For completeness, we include the chain configuration on step-A in this analysis, despite its negative hydrogen bond energy. Whether or not it is included has no effect on the overall conclusions.

In reviewing Fig. 8(b) several points become evident. First, an underlying commonality exists for hydrogen bonding in adsorbed water: the data fall on common curves for adsorption on terraces, steps or kinks, and in cluster or extended configurations. The trimer-open structure on step-A (1.69 Å, 0.07 eV) is the only significant outlier.

Second, the data fall into three distinct groups. The strongest

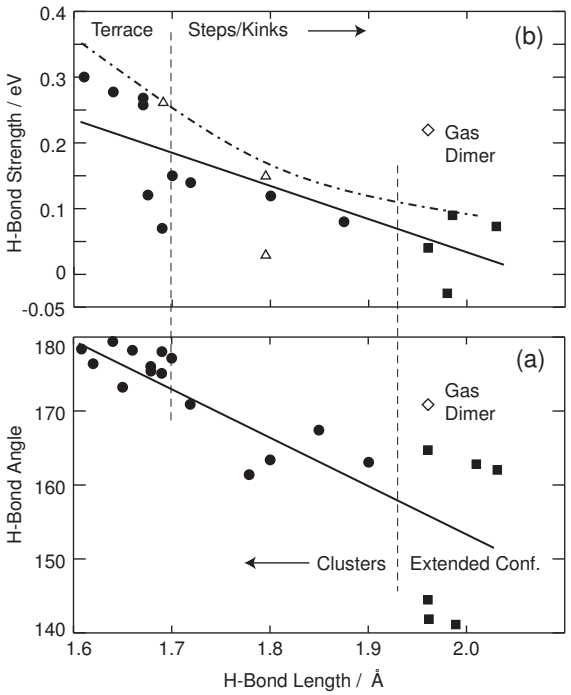

Figure 8: Correlation of hydrogen bond angles (a) and energies (b) with hydrogen bond lengths for adsorption of water on Pt terrace, steps, and kinks. Filled circles represent terrace and step/kink data. Filled squares represent extended configurations. The open diamonds represents data for the gas phase dimer. Open triangles represent data from ref. [19]. The dash-dot line represents hydrogen bond data for a variety of molecules taken from ref. [45]. The lines are least square fits to the filled data points.

hydrogen bonds of 0.26–0.30 eV and shortest bond lengths of 1.61–1.68 Å occur in clusters adsorbed at terrace sites. Intermediate hydrogen bond energies of 0.07–0.15 eV and bond lengths of 1.62–1.90 Å occur in clusters adsorbed at step and kink sites. The weakest hydrogen bond energies of −0.03 to 0.10 eV and longest bond lengths of 1.96 to 2.03 Å occur for the chain and zigzag extended configurations. Thus, hydrogen bond strength correlates with the nature of the surface, with strongest bonding occurring for adsorption at terraces and weaker hydrogen bonding for adsorption at step and kink sites. Hydrogen bonding is sensitive to the nature of the adsorbate with stronger bonds occurring in finite clusters and weaker bonds in extended configurations.

Third, the data can be related to other types of hydrogen bonding. The dash-dot line in Fig. 8(b) shows model results for hydrogen bond energy *vs.* hydrogen bond distance [45]. The model results were verified with data for ice, alcohols, carboxylic acid dimers, and oxalic acid. The model is in reasonably good agreement with the results presented here for adsorbed water.

Fourth, the data cannot be related, at least on an absolute basis, to hydrogen bonding in gas phase water. The bond energy correlation in part (b) lies well below the gas phase dimer point. At the gas phase bond length of 1.96 Å, the correlated bond energy for adsorbed water is approximately 0.08 eV. Alternatively, at the gas phase dimer bond strength of 0.22 eV, the correlated bond length of adsorbed water is 1.68 Å. An analogous relationship holds for the bond angle/bond length correlation in part (a). Hydrogen bonding in adsorbed water may be said to be "weaker" at a given bond length than in the gas phase, although stronger hydrogen bonds can be achieved at shorter bond lengths. The basis for this difference is most likely due to the interdependency of metal–water and hydrogen bond interactions discussed above.

4.2.3. Adsorbate-Adsorbate and Substrate-Adsorbate Interactions

The ratio of AA/SA interactions is highest for water clusters adsorbed on terrace sites (Table 3), in the range of 47% to 60% of the SA interactions. This shows that hydrogen bonding is important in establishing cluster stability. In contrast, the ratio of AA/SA interactions is less for adsorption on the stepped surfaces, ranging from 9% to 22% (excluding the chain configuration on step-A). Hydrogen bonding is not so important for adsorption at steps, which is in line with the hydrogen bond energy, length, and angle correlations displayed in Fig. 8.

Meng, et al. [19] used the same AA/SA ratio (Eq. 6) to characterize water interactions among several late transition and noble metal (111) surfaces. Their values were based on adsorbed hexamers. For Pt(111) they obtained a ratio of 0.9, which exceeds the highest ratio of 0.60 for the trimer on Pt(111) found in this study. Comparison of the two results suggests that hydrogen bond strength in the hexamer is further enhanced relative to that in the trimer.

5. Conclusions

DFT calculations were used to determine adsorption configurations and energies for water monomers, clusters, and extended configurations on Pt(111) terraces, (221) and (322) steps, and (763) and (854) kinks. Monomer water has a low adsorption energy, only 0.30 eV, on the (111) terrace, while dimers and trimers have stronger adsorption energies per water molecule of up to 0.48 eV, typical of those expected for water layers in general. Rotation of monomer, dimer, and trimer on the terrace is facile with energy barriers of 0.02 eV or less. Adsorption of monomers, dimers, trimers, and chain and zigzag configurations is stronger on the stepped and kinked surfaces than on the terrace, with per-molecule values ranging from 0.46 to 0.57 eV.

Hydrogen bond strengths were considered with respect to two reference states: adsorbed, non-interacting monomers (E_H) and a virtual state consisting of adsorbed, non-hydrogen bonded clusters ($E_{H,s}$). Only estimates of E_H are experimentally accessible, although hydrogen bond energy is averaged among all hydrogen bonds. Hydrogen bond energies $E_{H,s}$ referenced to the virtual state isolate water–water interactions from metal–water interactions. Such estimates are useful for dimers, but in trimers and more complex structures, they may be subject to inconsistency. All hydrogen bond strengths reported in this paper are E_H.

Hydrogen bonding plays a major role in water adsorbed on the (111) terrace with energies of 0.27 to 0.30 eV and ratios of AA to SA interactions of 0.47 to 0.6. In contrast, hydrogen bonding plays a minor role in adsorption on the stepped and kinked surfaces; hydrogen bond strengths are 0.22 eV or less and the ratios of AA to SA interactions are 0.3 or less. Hydrogen bond strength is correlated to hydrogen bond length with the strongest bonding occurring for the shortest bond. Water–metal interactions are the predominant component of the adsorption energy at steps and kinks. The reason for this is not increased coordination with the substrate atoms, as in metal on metal adsorption, because the water molecules adsorb ontop. The reason is that the less coordinated the substrate metal atoms are, the stronger the O-Pt interaction as evidenced by the low AA/SA ratio on step edges compared to the terrace. DFT/PW91 results appear to be in good agreement with experimental data, in particular the STM results of Morgenstern et al. [10] and adsorption experiment of Grecea et al. [23].

6. Acknowlegdements

Major funding for this work was provided by the Office of Naval Research and the National Science Foundation. A portion of the research was performed as part of an EMSL Scientific Grand Challenge project at the W. R. Wiley Environmental Molecular Sciences Laboratory, a national scientific user facility sponsored by the U.S. Department of Energy's Office of Biological and Environmental Research and located at Pacific Northwest National Laboratory. PNNL is operated for the Department of Energy by Battelle.

7. References

[1] P. Thiel and T. Madey, Surface Science Reports **7**, 211 (1987).
[2] M. Henderson, Surface Science Reports **46**, 5 (2002).
[3] A. Hodgson and S. Haq, Surface Science Reports **64**, 381 (2009).
[4] G. B. Fisher and J. L. Gland, Surface Science **94**, 446 (1980).
[5] S. Haq, J. Harnett, and A. Hodgson, Surface Science **505**, 171 (2002).
[6] J. L. Daschbach, B. M. Peden, R. S. Smith, and B. D. Kay, The Journal of Chemical Physics **120**, 1516 (2004).
[7] S. J. Suresh and V. M. Naik, The Journal of Chemical Physics **113**, 9727 (2000).
[8] A. Verdaguer, G. Sacha, H. Bluhm, and M. Salmeron, Chemical Reviews **106**, 1478 (2006).
[9] R. Pandit, M. Schick, and M. Wortis, Physical Review B **26**, 5112 (1982).
[10] M. Morgenstern, T. Michely, and G. Comsa, Physical Review Letters **77**, 703 (1996).
[11] A. Michaelides and K. Morgenstern, Nature Materials **6**, 597 (2007).
[12] K. Motobayashi, C. Matsumoto, Y. Kim, and M. Kawai, Surface Science **602**, 3136 (2008).
[13] A. Glebov, A. P. Graham, A. Menzel, and J. P. Toennies, The Journal of Chemical Physics **106**, 9382 (1997).
[14] K. Morgenstern, Surface Science **504**, 293 (2002).
[15] T. Mitsui, M. K. Rose, E. Fomin, D. F. Ogletree, and M. Salmeron, Science **297**, 1850 (2002).
[16] A. L. Glebov, A. P. Graham, and A. Menzel, Surface Science **427-428**, 22 (1999).
[17] A. Michaelides, A. Alavi, and D. King, Physical Review B **69**, 113404 (2004).
[18] A. Michaelides, V. Ranea, P. de Andres, and D. King, Physical Review Letters **90**, 216102 (2003).
[19] S. Meng, E. Wang, and S. Gao, Physical Review B **69**, 195404 (2004).
[20] P. J. Feibelman, Physical Review B **67**, 035420 (2003).
[21] V. Ranea, A. Michaelides, R. Ramirez, P. de Andres, J. Verges, and D. King, Physical Review Letters **92**, 136104 (2004).
[22] H. Ogasawara, B. Brena, D. Nordlund, M. Nyberg, A. Pelmenschikov, L. Pettersson, and A. Nilsson, Physical Review Letters **89**, 276102 (2002).
[23] M. Grecea, E. Backus, B. Riedmuller, A. Eichler, A. Kleyn, and M. Bonn, Journal of Physical Chemistry B **108**, 12575 (2004).
[24] G. Kresse and J. Hafner, Physical Review B **47**, 558 (1993).
[25] G. Kresse and J. Hafner, Physical Review B **49**, 14251 (1994).
[26] G. Kresse and J. Furthmuller, Computational Materials Science **6**, 15 (1996).
[27] G. Kresse and J. Furthmuller, Physical Review B **54**, 11169 (1996).
[28] J. P. Perdew and Y. Wang, Physical Review B **45**, 13244 (1992).
[29] D. Vanderbilt, Physical Review B **41**, 7892 (1990).
[30] G. Kresse and J. Hafner, Journal of Physics-Condense Matter **6**, 8245 (1994).
[31] G. Henkelman, B. P. Uberuaga, and H. Jonsson, Journal of Chemical Physics **113**, 9901 (2000).
[32] G. Henkelman and H. Jónsson, Journal of Chemical Physics **113**, 9978 (2000).
[33] Handbook of Chemistry and Physics, 78 ed., edited by D. Lide (CRC Press, Inc., New York, 1997-1998).
[34] B. Santra, A. Michaelides, and M. Scheffler, Journal of Chemical Physics **127**, 184104 (2007).
[35] T. van der Wijst, C. F. Guerra, M. Swart, and F. M. Bickelhaupt, Chemical Physics Letters **426**, 415 (2006).
[36] P. Vassilev, R. A. van Santen, and M. T. M. Koper, Journal of Chemical Physics **122**, 054701 (2005).
[37] D. Sebastiani and L. D. Site, Journal of Chemical Theory and Computation **1**, 78 (2005).
[38] R. Ludwig, Angewandte Chemie **40**, 1808 (2001).
[39] C. Burnham and S. Xantheas, Journal of Chemical Physics **116**, 1479 (2002).
[40] F. Sim, A. Stamant, I. Papai, and D. Salahub, Journal of the American Chemical Society **114**, 4391 (1992).
[41] R. Barnett and U. Landman, Physical Review B **48**, 2081 (1993).
[42] A. Michaelides, Faraday Discussions **136**, 2887 (2007).
[43] J. B. Li, Y. Li, S. L. Zhu, and F. H. Wang, Physical Review B **74**, 153415 (2006).
[44] J. Carrasco, A. Michaelides, and M. Scheffler, Journal of Chemical Physics **130**, 184707 (2009).
[45] E. Lippincott and R. Schroeder, Journal of Chemical Physics **23**, 1099 (1955).